XP-001120071 P.D.04-05-1997 P.110-117 (8)

NUMERICAL HEAT TRANSFER SIMULATIONS OF A VERTICAL BATCH FURNACE UNDER CLOSED-LOOP TEMPERATURE CONTROL

Gregory J. Wilson, Paul R. McHugh, and Robert A. Weaver
Semitool, Inc.
655 West Reserve Drive, Kalispell, MT 59901

Numerical heat transfer models of Semitool Express™ fast ramp batch furnaces for 200mm and 300mm wafers are run under multi-variable closed-loop temperature control. Predictions from these models are compared to furnace data obtained using the same controller. It is shown that these types of simulations help to characterize the thermal behavior of the furnace, evaluate new design concepts, and aid in controller development issues such as sensor placement.

INTRODUCTION

Time dependent computational models of a batch furnace under closed-loop temperature control are useful for characterizing the thermal environment of the furnace, evaluating new design concepts, and developing controllers. The approach of the present effort is to use two different thermal models; a relatively simple model that is computationally inexpensive and a complex model that, although more expensive to run, is more accurate. The simple model is useful for development of the numerical tools and for parametric studies. The complex model allows investigation of detailed design issues. Two different furnaces are modeled in this paper. One is the Semitool Express™ 200mm-wafer furnace with 7 heating zones and the other is the Express™ 300mm-wafer furnace with 9 heating zones. Besides size differences, a major distinction between the two furnaces is the inclusion of a base heater in the 300mm furnace.

COMPUTATIONAL MODELS

The axisymmetric furnace simulations in this work employ a research code called TWAFER (1) and a commercial computational fluid dynamics software package called CFD-ACE (2). TWAFER assumes a batch furnace geometry and includes diffuse, gray radiation heat transfer using view factors, as well as heat conduction through solid materials. The TWAFER model of the Semitool Express™ 200mm-wafer furnace is presented in Fig. 1. Major components of the model are the individual silicon wafers (56 wafers in this case), semi-transparent quartz liner and process jars, resistive heater, and insulation. The insulation is an important component of the model because it determines the heat loss of the system and, thus, the steady state power requirements of the furnace. The CFD-ACE package allows an arbitrary geometry defined with a non-orthogonal, finite-volume mesh. The furnace model developed with this code is presented in Fig. 2. This model allows an accurate geometric representation of the quartz jars, pedestal, and base plate. Diffuse, gray radiation and heat conduction through solids are included just as in TWAFER, but the radiation model is based upon the discrete ordinate method. The enlarged view in Fig. 3 of the CFD-ACE model near the center of the wafer stack shows that it has all of the same major components present in the TWAFER model. Figure 3

also shows that the grid density is decreased when moving from the wafer stack (where points are needed to resolve the individual wafers) out to the insulation. This technique reduces the number of grid points in the model by approximately one third. The CFD-ACE model contains approximately 20,000 cells compared to approximately 600 cells in the TWAFER model. The input to both models is power provided to each of the independent heater zones.

The CFD-ACE model geometry in Fig. 2 depicts the thermocouple sensor locations used to control temperature within the furnace. Sensors adjacent to the heater zones are referred to as spike thermocouples while those near the wafers are called profile thermocouples. There is one spike/profile thermocouple pair assigned to each heater zone. The numerical simulations do not explicitly model the sensors but use heater and wafer temperatures from cells nearest to the spike and profile sensor locations. This is a good approximation for steady-state simulations but may introduce errors during transients since the thermal response of the sensors can be different from that of the heaters or wafers. Inclusion of two sets of sensors (i.e., profile and spike) enables implementation of several different furnace temperature control strategies. For example, control may be based solely upon feedback from either spike or profile thermocouple measurements, or control may be accomplished by using cascaded feedback loops containing both spike and profile information. The results of this study employ either spike or profile control, but not cascade control.

Figure 4 depicts a CFD-ACE model of the nine-heater-zone Express™ 300mm-wafer furnace. A base heater has been incorporated into this design to add heat to the cooler region that occurs near the bottom center of the furnace, thereby increasing the area within the furnace where precise temperature control is possible. The presence of the base heater also reduces the power requirements on the bottom side-heating element (zone 8). Previous simulations under closed-loop temperature control assisted in evaluating potential base heater designs by investigating the effect of the base-heater height, angle, and power density. Alternate profile sensor locations for zones 1 and 8 are considered in this model, as marked in Fig. 4. Reasons for considering these alternate locations are discussed later in the paper.

MULTI-VARIABLE CONTROLLER METHODOLOGY

The heat transfer algorithms of TWAFER and CFD-ACE are coupled with a Linear Quadratic Gaussian (LQG) control strategy (3). The LQG controller used here utilizes integral action (4), and integral reset (5) to improve controller performance. The LQG controller was designed and tested within the MATLAB (6) software environment. Coupling of the controller to the CFD-ACE code was accomplished through CFD-ACE user-subroutines that are compiled and linked to the CFD-ACE executable. A similar approach was used to couple the controller to the TWAFER code. However, the availability of the TWAFER source code and its quick execution time enabled the coupling to reside within MATLAB. At each time step in the heat transfer simulation, temperatures and set point information from the model (i.e., either TWAFER or CFD-ACE) are delivered to the control algorithm, which then returns the new heater power values to the model. Linear models used for the controller design were initially constructed via an open

loop characterization of the nonlinear CFD-ACE model in a fashion similar to that described by Spenc et al. (7). This characterization consisted of starting the CFD-ACE model at a steady-state and then sequentially perturbing individual power zones, while recording both the commanded power and the computed wafer temperatures. Open-loop characterization runs of this sort work well when using numerical simulations, but may not work as well when characterizing a real furnace. Furnace temperatures during an open loop test may tend to drift away from the desired characterization temperature due to slow residual transients or unexpected system disturbances. This tendency motivates running furnace characterization tests under closed-loop temperature control. However, open-loop simulation data (i.e., from either TWAFER or CFD-ACE) can still be used to build the initial controller that is used during the furnace test. This procedure was adopted here along with the use of a Pseudo-Random Binary Sequence (PRBS) algorithm to adjust set points during the closed-loop furnace characterization test, which was run under spike control. This data was then used to build a linear state space model of the furnace using the MATLAB System Identification Toolbox.

RESULTS

The agreement between TWAFER and CFD-ACE predictions and 200mm-wafer Express™ furnace data was evaluated using pulse-train tests run under spike control. Selected results from these tests are presented in Figs 5 through 9. The same spike LQG controller was used in each case. This controller operated with a 1 second sample rate and was derived from furnace data as described above. The methodology used in collecting the data consisted of first stabilizing the system at 800°C. Afterwards, under spike control, the set points for each zone were sequentially perturbed from 800°C to 810°C. The duration of these pulses was 10 minutes, followed by a 10 minute period where the set points were returned to 800°C. This data serves to reveal system response characteristics as well as the agreement between the furnace data and the simulation data. Figure 5 presents the furnace spike thermocouple measurements and the CFD-ACE and TWAFER heater element temperature predictions. The spike response characteristics are similar but the model predictions are smoother. Of particular interest are the wafer temperatures within the furnace. Figure 6 presents the zone 4 wafer measurement during the pulse train. Reasonable agreement is obtained using both CFD-ACE and TWAFER, although TWAFER over-predicted the zone 4 response when the zone 4 spike set point was perturbed. CFD-ACE captured the smaller zone-to-zone interactions better than TWAFER. Larger differences between the simulations and the measurements were observed near the ends of the wafer load, i.e. zone 1 and zone 7, as can be seen in Fig. 7. At the bottom of the load (zone 7), the simulations tend to over predict the measurements, while at the top of the load (zone 1) the model predictions tend to under predict the profile thermocouple measurements. Note, however, that reasonable agreement (i.e., within several degrees) is still seen between the furnace data and the simulation data. The dynamic responses of the furnace measurements and the simulations were similar, with CFD-ACE again able to better capture the smaller zone-to-zone interactions. Comparisons of the power responses are shown in Figs. 8 and 9. The agreement between the power responses near the middle of the furnace (Fig. 8) was good, whereas near the ends (Fig. 9) significant power level offsets were observed, although the dynamic responses were similar. The most significant power level difference occurred in zone 7,

where the furnace required an additional 1000W of power. Similar differences have also been observed between the first generation furnace design used in this study and the current furnace design. One significant modification in the current design is the elimination of potential natural convection flow paths, e.g., flows between the element and the liner jar. Note that the simulations do not consider convective heat losses (i.e., either forced or free convection). Recent runs using the current furnace design, operating under spike control at 800°C, found that zone 7 delivered 1572.3W of power, in sharp contrast to the 2570W required in Fig. 9. This value also agrees more closely with the CFD-ACE and TWAFER predictions of 1463.3W and 1646.1W, respectively. Other possible explanations for the differences observed between the furnace data and the simulation data include:

1. Furnace measurements are based upon thermocouple readings that are not precisely located either on the heater element or on the wafers themselves, and whose dynamic response is not modeled.
2. The heater element is modeled a simple heat source.
3. Significant heat loss uncertainties exist, especially near the ends of the furnace.
4. Uncertainty exists in material properties, especially radiative properties. In this study material properties were assumed to be independent of temperature.

Considering the difficulties enumerated above, it is felt that the model predictions are accurate enough to be used for qualitative engineering judgments/evaluations and for preliminary control system design/evaluation. In fact, conducting simulations under closed-loop control helps compensate for some model inaccuracies by allowing the control system to adjust power levels just as an operating temperature control system is expected to adjust to differences between furnaces, or to changes that occur in a given furnace over time, e.g. due to aging furnace components or the introduction of replacement parts. Conducting simulations under closed-loop temperature control also helps identify discrepancies between furnace data and model predictions. Because furnaces typically operate under closed-loop temperature control, simulation data collected under similar conditions is more amenable to data comparisons. Additionally, trial-and-error selection of power input values necessary to yield a desired process temperature is difficult.

CFD-ACE profile temperatures and powers from a simulated ramp for the 300mm furnace model are shown in Figs. 10 and 11, respectively. Profile temperature control was used during the simulation, with a 5 second sample rate to reduce execution time. A second order ramp set point trajectory was used with a maximum rate of 50 degrees/min. The base heater power was limited to 3 kW, while the other heater zones were limited to 7.45 kW. Note from Fig. 11 that during the first 500 seconds, all the heater zones except zone 1 saturated, resulting in a temperature spread of about 60°C with the control point of the base heater zone lagging the farthest behind. After approximately 500 seconds the power zones unsaturated, causing the separation to diminish. The control point temperatures were within 0.5 degrees of the set point at the end of the ramp, but unfortunately with zone 7 delivering no power. Initial 300mm pulse-train data, represented by the solid lines in Fig. 12, indicated that the problem was due to the existence of strong coupling between zones 7 and 8. This information suggested lowering the zone 8 control point to the alternative point located in Fig. 4. A similar problem can

be identified in Fig. 12 for the zones near the top of the furnace, which motivated consideration of the alternate location for the zone 1 control point as well. Evidence that these new locations helped to decouple these problem zones is demonstrated by the dashed lines in Fig. 12, which show reduced profile temperature responses due to spike perturbations in adjacent zones. These new locations enabled improved furnace controllability without compromising wafer temperature uniformity.

Figure 13 compares axial wafer load uniformity, as measured by wafer edge temperatures, for two potential 300mm designs. The first design used the solid-symbol control point locations indicated in Fig. 4 and a clear quartz pedestal top. The second design used the alternate control point locations for zone 1 and zone 8, and also a silicon carbide pedestal top. The second design resulted in significantly better wafer temperature uniformity near the bottom of the wafer load. Also improved was furnace temperature controllability due to the use of the alternate control points. This improvement was reflected in more accurate temperature control that avoided zero-power saturation at the set point temperature. For example, the second design achieved temperature stabilization within 0.02 degrees of the set point with zone 7 delivering 305.8 W, as compared to the 0.5 degree variation seen using the first design with zone 7 delivering no power.

CONCLUSIONS

Complex heat transfer models of the Semitool Express™ Fast Ramp vertical batch furnace have been successfully coupled to an LQG controller and used in an engineering R&D environment. These simulations add insight into the thermal characteristics of the furnace and provide a tool for furnace and control system design. Because the detailed model simulations are computationally expensive, the development of these tools was greatly aided by use of the TWAFER code, a simpler and much faster thermal model.

ACKNOWLEDGMENTS

The authors would like to thank Bill Houf and Paul Spence at Sandia National Laboratories, Livermore CA. for many helpful discussions. The technical support provided by CFD Research Corporation, and the furnace time and assistance provided by the Laboratory staff of Semitool's Thermal Products Division are greatly appreciated.

REFERENCES

1. W.G. Houf and J.F. Grear, *J. of Mat. Sci. and Eng.* **B17**, pp. 163-171 (1993).
2. *CFD-ACE Graphical User Interface Manual*, Version 2.0, GR-96-4, CFD Research Corporation, Huntsville, LA (1996).
3. P. Dorato, C. Abdallah and V. Cerone, *Linear-Quadratic Control, An Introduction*, Prentice Hall, Englewood Cliffs, NJ (1995).
4. J. Ebert, et al., "Thermal Modeling and Control of Rapid Thermal Processing Systems," WP10 5:10, Proceedings of the 34th Conference on Decision & Control, New Orleans, LA. (1995).
5. C.F. Elia, "RTP Multivariable Temperature Controller Development," WP4 5:40, Proceedings of the American Control Conference, Baltimore MD (1994).

6. *MATLAB, High-Performance Numeric Computation and Visualization Software: User's Guide*, The MathWorks, Inc., Natick, MA (1996).
7. P. Spence, et al., "Process Control of Large-Scale Finite Element Simulation Software," SAND96-8214, UC-405, Livermore, CA (1996)
8. L. Ljung, *System Identification: Theory for the User*, Prentice Hall PTR, Upper Saddle River, NJ (1987).

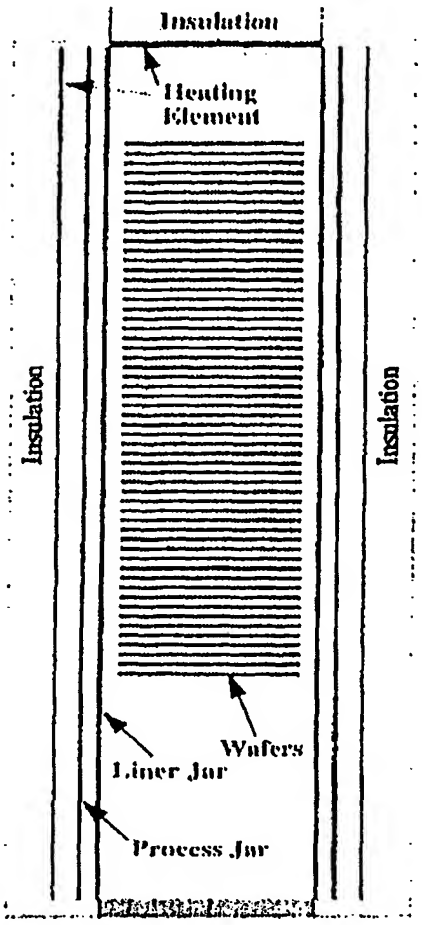

Fig 1. TWAFER model of Express 200mm-wafer furnace.

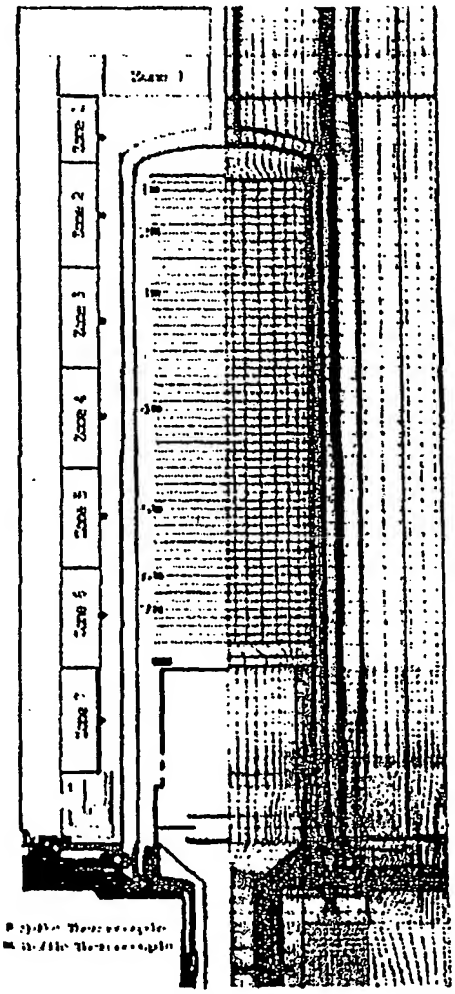

Fig. 2. CFD-ACE model geometry and mesh for the 200mm-wafer furnace.

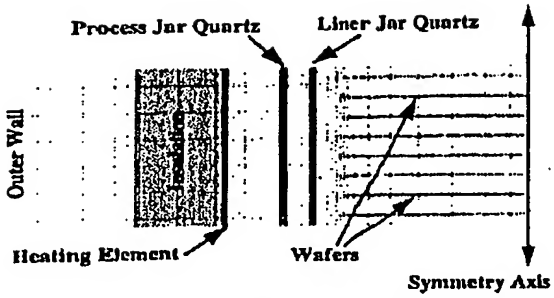

Fig. 3. Enlarged view of the CFD-ACE model geometry and mesh.

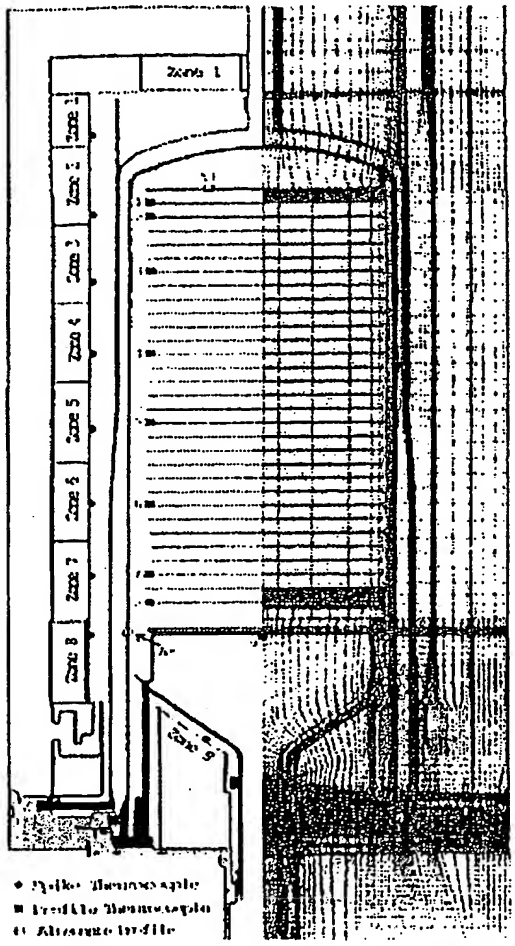

Fig. 4. CFD-ACE model geometry and mesh for the 300mm-wafer furnace.

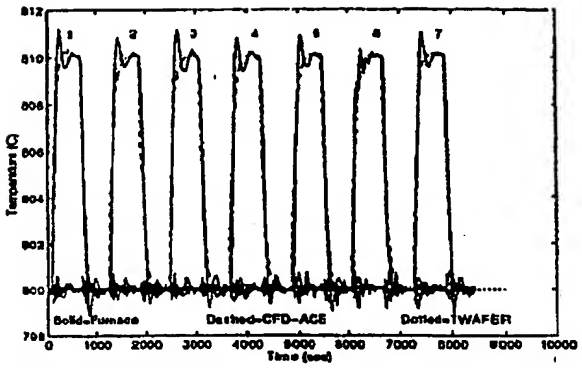

Fig. 5. Spike temperature responses during pulse-train tests.

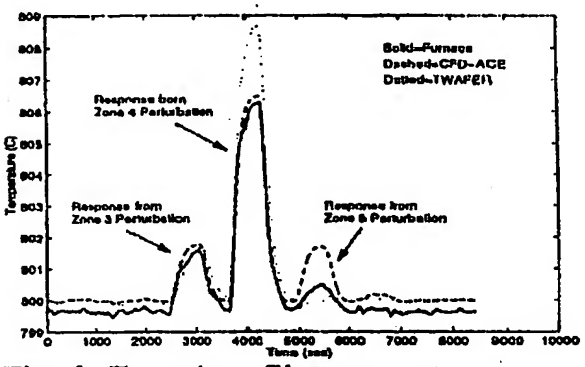

Fig. 6. Zone 4 profile temperature responses during pulse-train tests.

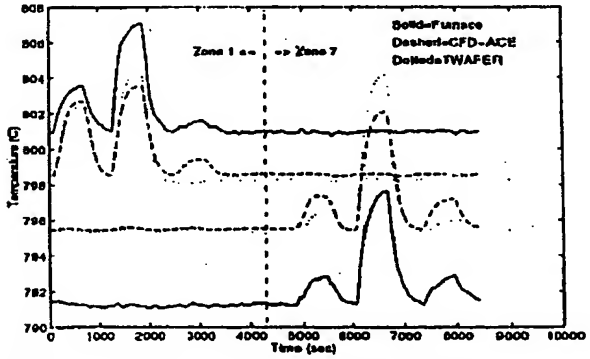

Fig. 7. Zone 1 and Zone 7 profile temperature responses during pulse-train tests.

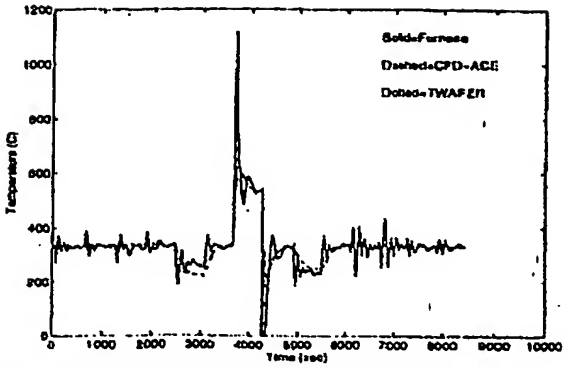

Fig. 8. Zone 4 power values during pulse-train tests.

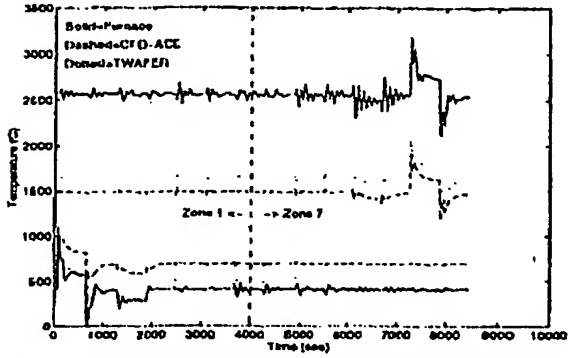

Fig. 9. Zone 1 and Zone 7 power levels during pulse-train tests.

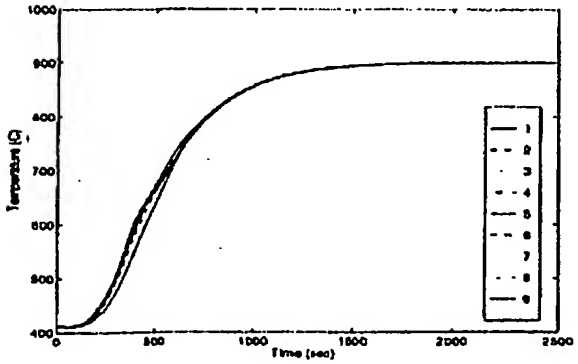

Fig. 10. CFD-ACE profile temperature predictions during ramp.

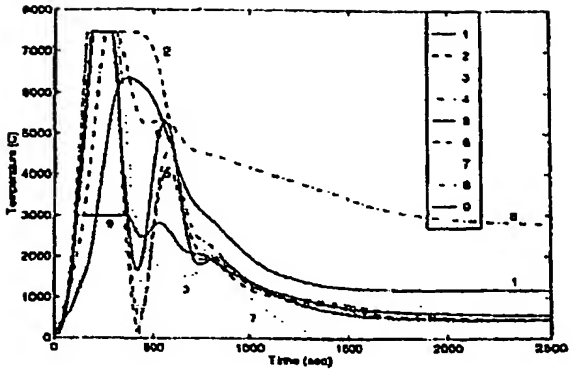

Fig. 11. CFD-ACE zone power predictions during ramp.

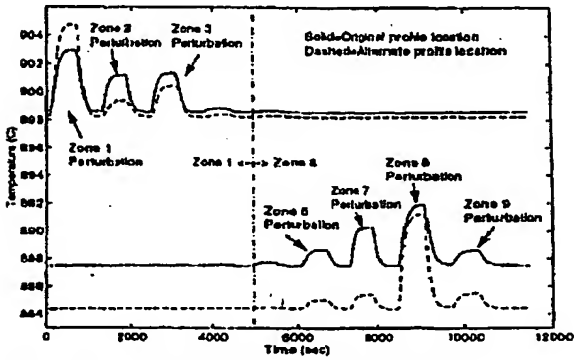

Fig. 12. CFD-ACE predicted Zone 1 and Zone 8 profile temperatures during pulse-train tests with two 300mm furnace designs.

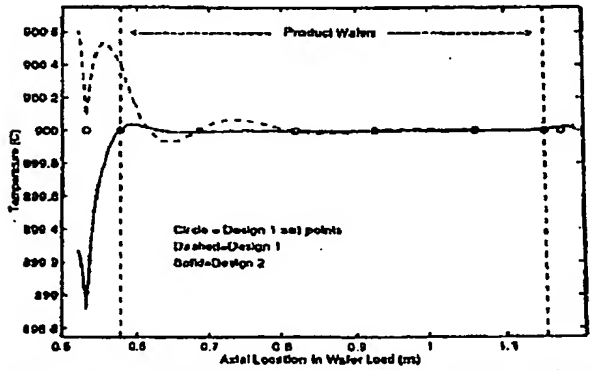

Fig. 13. CFD-ACE predicted wafer-edge temperatures for two 300mm furnace designs.